

# Influence of grain size and degree of crystallization of intergranular glassy phase on the mechanical behaviour of a debased alumina

N. P. PADTURE, H. M. CHAN

*Department of Materials Science and Engineering, Lehigh University, Bethlehem, PA 18015, USA*

The influence of microstructure on the crack resistance (*R*-curve) behaviour of a commercial debased alumina containing large amounts of glassy phase (28 vol%) has been studied by strength measurements at controlled flaw sizes produced by indentation. Both the individual and combined effects of (a) grain size, and (b) intergranular second phase (glassy or crystalline) were evaluated. Enhancement of the *R*-curve behaviour was observed when the average grain size was increased from 3–18  $\mu\text{m}$  by thermal treatment. However, no effect of the degree of crystallinity of the intergranular second phase on the *R*-curve behaviour, in either small- or large-grained materials, was observed. These results are discussed with reference to the influence of grain-boundary residual stresses on grain bridging across the crack interface.

## 1. Introduction

In recent years there has been increasing evidence that non-transforming ceramics such as aluminas can exhibit so-called *R*-curve behaviour, i.e. they show increasing toughness with increase in crack size [1–6]. The enhancement of *R*-curve behaviour yields several tangible benefits. Firstly, the ceramic exhibits a range of flaw sizes over which the strength is near-invariant. In turn, this “flaw tolerance” enables the engineer to work with a single (flaw-size independent) design stress. The advantage from the ceramics processing standpoint is that the strength of a ceramic with strong *R*-curve behaviour is relatively insensitive to processing defects. In addition, it has recently been postulated that enhanced *R*-curve behaviour results in an increase in the Weibull modulus [7–9].

Because it has been clearly demonstrated that the extent of the *R*-curve behaviour is influenced by microstructure [3], it would seem highly feasible to modify *R*-curve characteristics through control of microstructural variables. The microstructural parameters evaluated in this study were (a) grain size, and (b) degree of crystallinity of the intergranular phase. The selection of these particular parameters was based on the consideration of a model which assumes grain-localized bridging in the crack wake [1, 5, 10]. In the above model, represented schematically in Fig. 1, the grains bridging the crack are “clamped” in the matrix by compressive residual stresses arising from thermal expansion anisotropy [11]. These grains thereby exert a restraint across the crack walls, giving rise to increased toughness in a manner analogous to that

of fibre-reinforced composites. Without going into the details of the stress-displacement relation for the bridge elements [11, 12], it can be appreciated that the degree of enhanced toughening will depend both on the grain size (which determines the length over which the grains must be pulled out), and the residual stresses (which control how tightly the grains are clamped).

A limited number of systematic experimental investigations of these predictions have been carried out, and these confirm a strong dependence on grain size. A study on nominally single-phase aluminas showed that coarsening the microstructure results in a stronger *R*-curve [3]. Similar results were obtained for a debased alumina (containing 18 vol % intergranular phase) [13]. The influence of the intergranular second phases, however, is less well documented, and different studies have produced somewhat conflicting results. Thus several researchers [14–18] have reported significant increases in the toughness values of liquid-phase-sintered aluminas containing 10–30 vol % intergranular glass. The toughness improvements resulted from simple heat treatments, and were attributed to crystallization of the glass. However, it should be noted that the toughness measurements in those studies were performed at a single crack length. In contrast to this, work by Bennison *et al.* [13] showed that for fine-grained aluminas containing 18 vol % second phase, crystallization of the second phase had very little effect on the crack resistance curve. Powell-Doğan and Heuer [19] also showed that for 96% alumina, crystallization of the second

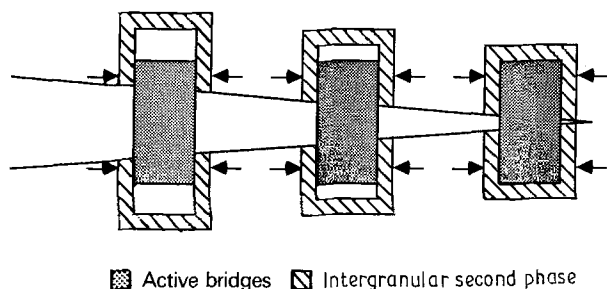


Figure 1 Schematic representation of grain-localized bridging of the crack.

phase had no effect on either the mechanical properties, or the mode of fracture.

The purpose of this study was to determine experimentally the relative influence of these two variables, grain size and second phase, on the *R*-curve behaviour of a debased alumina. This work differs from that of previous researchers in that both the individual and combined influence of grain size, and crystallinity of the second phase, are determined.

## 2. Experimental procedure

Some 300 specimens of a commercial debased (liquid-phase sintered) alumina (AD 85) in the form of discs (25 mm diameter  $\times$  3 mm) were obtained. A series of heat treatments was carefully devised to produce four sets of specimens of differing microstructures. Table I shows the details of the heat treatments and the resulting microstructures. The notation S or L refers to "small" or "large" grain size, respectively, and C or G refers to crystalline or glassy second-phase, respectively.

Specimens for transmission electron microscopy (TEM) were prepared following standard procedures for ceramic materials. Discs (3 mm) were ultrasonically cut from thin sections of the above samples. The discs were then dimpled to a thickness of 20  $\mu$ m in the centre and ion-beam milled until perforation. Subsequent investigation on the transmission electron microscope was carried out at an accelerating voltage of 120 keV. The chemical composition of the intergranular glass was determined using energy dispersive spectroscopy of X-rays (EDS) on the same instrument. A "standard" glass (SRM 2063) of known composition was used to provide the necessary *k*-factors for compositional analysis. Samples were prepared for scanning electron microscopy (SEM) by polishing sections

to 1  $\mu$ m grade followed by thermal etching at 1500  $^{\circ}$ C for 15 min.

Mechanical testing of AD85-S-G, AD85-S-C, AD85-L-G and AD85-L-C was carried out as follows. About 50 disc specimens of each batch were polished to 1  $\mu$ m grade on the prospective tensile side. A Vickers indentation was made at the centre of the polished surface with loads varying from 2–300 N. Some samples were left unindented. All indentations were made in air and the samples allowed to stand for 10 min. A drop of vacuum grease was then placed on the indentation sites. The specimens were broken in biaxial flexure using the three-point support and punch fixture [20], and failure times were kept below 20 ms to minimize effects from static fatigue. Strength values were calculated from the breaking loads and specimen dimensions using thin-plate and beam formulas [21]. Care was taken to examine all specimens after fracture to verify the indentation site as the origin of failure. The specimens that did not fracture from indentations were incorporated into the data pool for unindented controls. Details of this particular method of mechanical testing have been described elsewhere [3].

Preliminary experiments revealed that crystallization of the intergranular glass produced predominantly anorthite ( $\text{CaO} \cdot \text{Al}_2\text{O}_3 \cdot 2\text{SiO}_2$ ). To obtain a comparison between the high-temperature mechanical properties of anorthite and alumina, the hardness of bulk anorthite was determined as a function of temperature from 20–1200  $^{\circ}$ C. Bulk anorthite was made by first melting anorthite composition glass from reagent grade  $\text{SiO}_2$ ,  $\text{Al}_2\text{O}_3$  and  $\text{CaCO}_3$  raw materials in a Pt–Rh crucible at 1600  $^{\circ}$ C for 24 h. This was followed by crystallization at 1200  $^{\circ}$ C for 30 min.

## 3. Results

### 3.1. Microstructure

Table II shows the composition of the intergranular glass of AD85-S-G samples after homogenization heat treatment, as determined by X-ray EDS. The values represent an average of ten different spectra obtained from different regions of the sample. The compositions were observed to be consistent within  $\pm 5\%$ , implying that the glassy phase is homogeneous. In addition, the glass composition obtained was found to agree within  $\pm 5\%$  of the values determined by Wiederhorn *et al.* [22] for AD85 with the same heat treatment. Using this composition as a basis, the heat treatment

TABLE I Heat-treatment schedules and microstructures

Material	Heat treatment	Purpose	Resulting microstructure	
			Grain size ( $\mu$ m)	Intergranular phase
AD85-S-G	As-received	Homogenize intergranular glass	3	Glassy
AD85-S-C	(a) 1400 $^{\circ}$ C for 6 h (quenched) (b) 1150 $^{\circ}$ C for 130 h		3	Partially crystalline
AD85-L-G	(a) 1550 $^{\circ}$ C for 250 h	Increase grain size	18	Glassy
AD85-L-C	(a) 1550 $^{\circ}$ C for 250 h (b) 1200 $^{\circ}$ C for 130 h	Crystallize inter-granular glass with large grain size	18	Partially crystalline

TABLE II Average composition (wt %) of the intergranular glass in AD85

SiO <sub>2</sub>	Al <sub>2</sub> O <sub>3</sub>	MgO	CaO	BaO
56.5	27.5	2.1	8.6	5.3

given in Table I was devised in order to obtain anorthite as the major crystalline phase [23].

Fig. 2 shows scanning electron micrographs of AD85-S-G (grain size  $\approx 3 \mu\text{m}$ ) and AD85-L-G (grain size  $\approx 18 \mu\text{m}$ ). Qualitative visual comparison of the two micrographs shows that the heat treatment results in a scaling up of the grain structure as a whole, and that there is no significant change in the distribution of grain sizes about the mean. Fig. 3a and b show transmission electron micrographs of AD85-S-G and AD85-S-C depicting glassy and crystalline intergranular phases respectively. The grain size has not changed appreciably during crystallization heat treatment. The crystalline intergranular phase in AD85-S-C is observed to be mostly anorthite. With this composition it was not possible to achieve 100% crystallinity; thus pockets of residual glassy phase were observed at many triple points. From TEM examination, the overall degree of crystallinity was estimated to be  $\approx 80\%$ .

### 3.2. Mechanical behaviour

Fig. 4 shows indentation load versus failure stress for the four sets of samples. Consider firstly the behaviour of the fine-grained material. It can be seen that the data points for AD85-S-G and AD85-S-C lie essentially on the same line. The results for the coarse-grained specimens (AD85-L-G and AD85-L-C), on the other hand, fall on a distinctly separate curve.

The results of the hot-hardness measurements obtained from the bulk anorthite samples are shown in Fig. 5. Data for alumina [24] are also plotted for comparison. Although the hardness of anorthite at

room temperature is significantly lower than that of alumina, its rate of decrease with increasing temperature is lower. Consequently, at temperatures around 1000 °C, the hardness values of the two phases are similar.

### 4. Discussion

The results depicted in Fig. 4 clearly show that *R*-curve behaviour, as evinced by the flattening of the data in Fig. 4 at low indentation loads, is enhanced with increasing grain size. This behaviour is consistent with the observations of other researchers obtained on both single-phase [3, 25] and two-phase aluminas [3, 13]. It confirms grain size as a significant parameter in determining the extent of increased toughening with crack extension.

However, the effect of crystallization of the intergranular phase on the *R*-curve properties of these materials appears to be insignificant. In terms of the grain-bridging model, this null effect may seem surprising, because the bridging processes are thought to be sensitive to residual stresses,  $\sigma_r$ , in the grain-boundary regions. To explore the validity of this reasoning further, the magnitude of these grain-boundary stresses due to thermal expansion anisotropy between the alumina (A) and the intergranular anorthite (An) can be estimated from the following relation for a spherical inclusion embedded in a matrix [26, 27]

$$\sigma_r = [(\alpha_A - \alpha_{An})\Delta T]/[(1 + \nu_A)/2E_A + (1 - 2\nu_{An})/E_{An}] \quad (1)$$

where  $\alpha$  is the linear thermal expansion coefficient,  $\nu$  is Poisson's ratio,  $E$  the elastic modulus and  $\Delta T$  is the difference between heat treatment and ambient temperatures. Although the inclusion problem represents an oversimplification of the experimentally observed

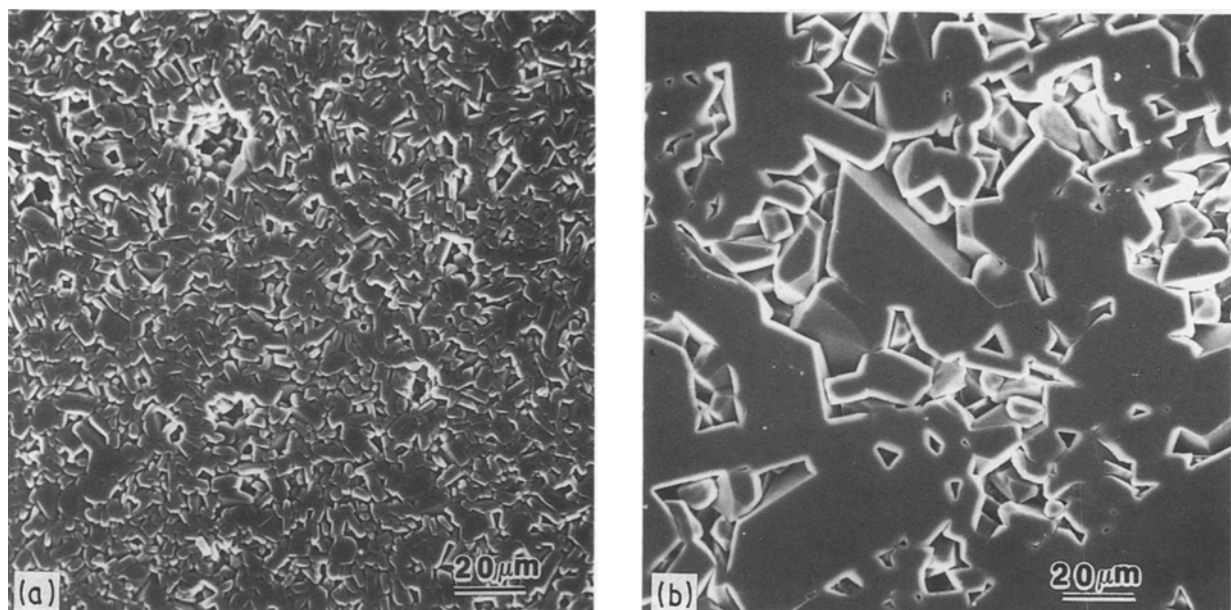


Figure 2 SEM secondary electron images of polished and etched sections of AD85 aluminas (a) AD85-S-G (fine-grained material), (b) AD85-L-G (coarse-grained material).

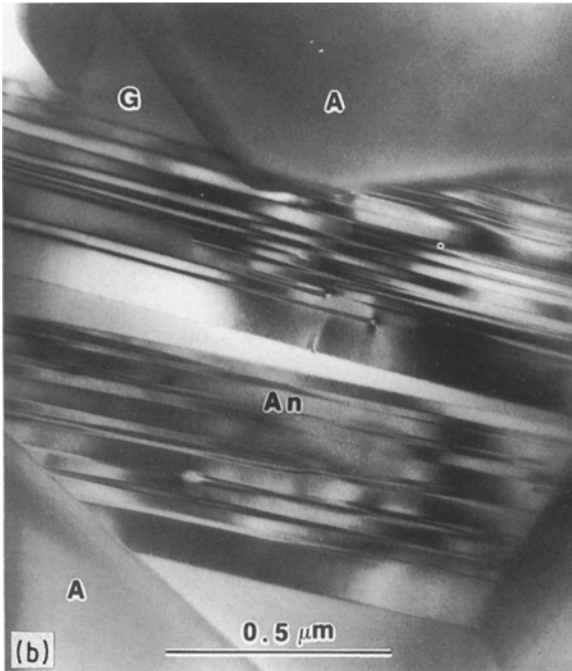
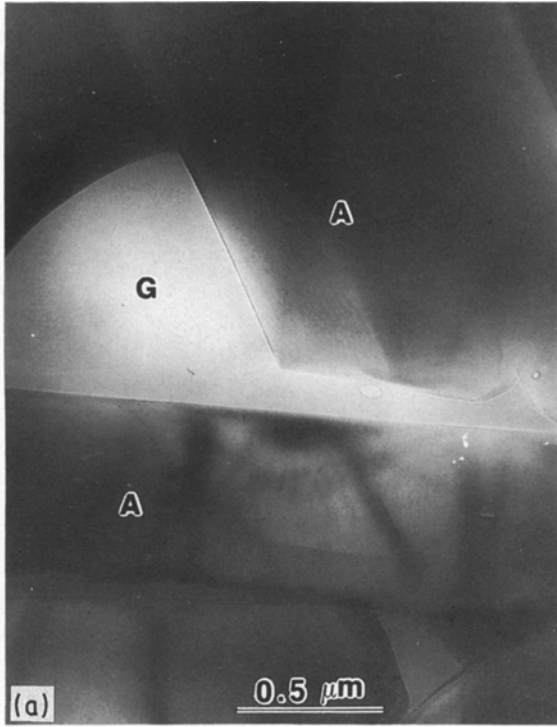


Figure 3 TEM bright-field images of AD85 aluminas (a) AD85-S-G showing intergranular glassy pockets (A, alumina; G, glass), (b) AD85-S-C showing crystalline intergranular phase (A, alumina; An, anorthite; G, residual glass).

morphology, it is believed that this relation gives a useful indication of the magnitude of the residual stresses. Taking  $\alpha_A = 9.0 \times 10^{-6} \text{ }^\circ\text{C}^{-1}$  [28],  $\alpha_{An} = 3.7 \times 10^{-6} \text{ }^\circ\text{C}^{-1}$  [29]\*,  $E_A = 390 \text{ GPa}$  ( $\nu_{Al} = 0.2$ ) [3],  $E_{An} = 250 \text{ GPa}$  ( $\nu_{An} = 0.25$ ) [30] and  $\Delta T = 1000 \text{ }^\circ\text{C}$ , we obtain  $\sigma_r = 1.5 \text{ GPa}$  for the alumina/anorthite system. For a single-phase alumina, taking  $\alpha_{Lc} = 8.6 \times 10^{-6} \text{ }^\circ\text{C}^{-1}$  and  $\alpha_{llc} = 9.6 \times 10^{-6} \text{ }^\circ\text{C}^{-1}$  [28], we ob-

\* It should be noted that alumina and anorthite are non-cubic materials and possess thermal expansion anisotropy along  $a$  and  $c$  axes. Because the thermal expansion anisotropy within these individual crystals is much less than that between the two phases, the values mentioned here are average and represent the thermal expansion coefficients of polycrystalline materials.

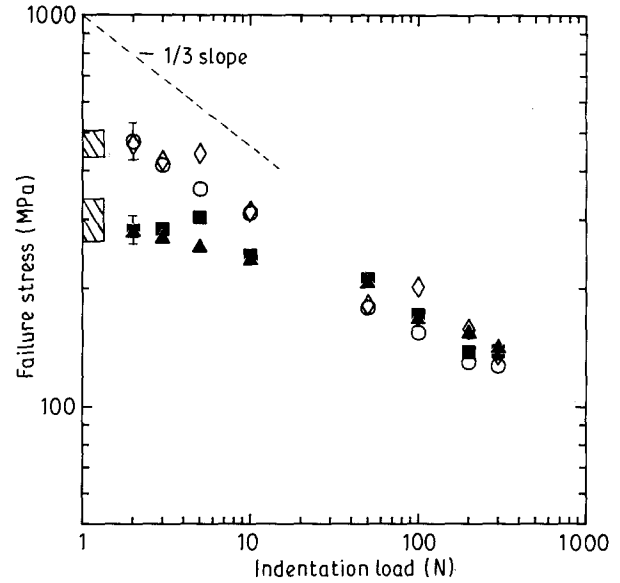


Figure 4 Plot of indentation load versus failure stress for four different materials, derived from AD85. The hatched region represents failures from natural flaws. (Representative error bars are included on the end data points.) (○) AD85-S-G, (◇) AD85-S-C, (■) AD85-L-G, (▲) AD85-L-C.

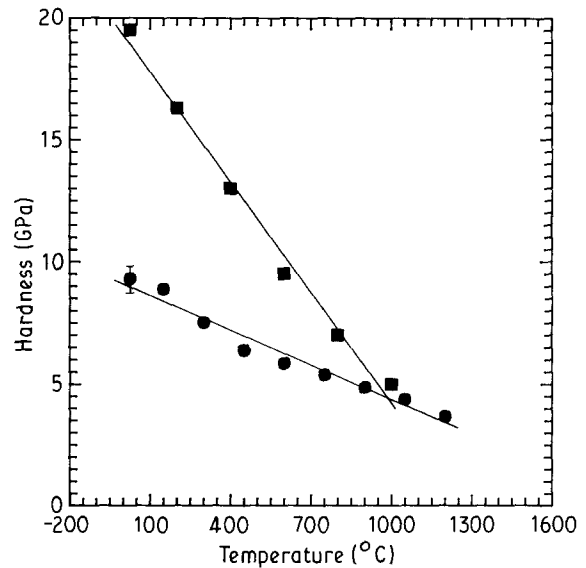


Figure 5 Comparison of hardness as a function of temperature between (■) alumina [24] and (●) anorthite (present work). (A representative error bar is shown on the end data point.)

tain  $\sigma_r = 0.35 \text{ GPa}$ . Thus the residual stresses induced in the two-phase alumina are greater, by about a factor of four, than in the single-phase material.

One could therefore argue that the  $R$ -curve in single-phase alumina should be further enhanced in the two-phase alumina with the crystalline second phase. That this was not observed experimentally, suggests that the residual stresses must be at least partially relaxed in AD85-S-C and AD85-L-C. As described previously, TEM examination of these samples revealed that the anorthite was highly twinned. In addition, residual glass was often observed in the

intergranular pockets. It is arguable, therefore, that relaxation of the grain-boundary residual stresses is taking place at the treatment temperature by deformation of either the anorthite or glassy phase. Because no dislocation activity was observed in the alumina grains, deformation of the alumina grains was disregarded as a possibility. Consideration of Fig. 5 shows that deformation of the anorthite appears less likely, because at elevated temperatures the hardness values of alumina and anorthite become comparable, so it is difficult to see why the anorthite would deform in preference to the alumina.

This essentially leaves the role of the residual glass to be considered. Because the approximate composition of the glass is known, it is possible to estimate the value of the glass viscosity from standard data [31]. For comparable glass compositions, the softening temperature, i.e. the temperature at which the glass will deform appreciably under its own weight, is 900°C. Thus at the level of stresses which have been calculated, the glass would be expected to flow readily. It is therefore suggested that the expected change in mechanical properties does not occur because of relaxation of the induced stresses by viscous flow of the residual glass.

The above discussion represents a highly simplified picture of the deformation processes which take place on cooling of the crystallized AD85 to ambient temperatures. Nonetheless, the postulate that the induced stresses are being relaxed is consistent with the experimental data. Ideally, it would have been desirable to estimate the stress distribution within the microstructure more accurately, by taking into account the morphology of the various phases. Unfortunately, the complexity of the microstructure of the commercial materials studied rendered such analysis intractable. It is envisaged that laboratory-processed specimens with controlled microstructures will be more amenable to theoretical modelling. Work is thus currently under way to process two-phase aluminas where the glass composition is controlled so that virtually 100% crystallinity can be achieved.

## 5. Conclusions

For the commercial liquid-phase-sintered aluminas examined in this study, the effect of grain size on the *R*-curve behaviour predominates. Crystallization of the intergranular glass had relatively little to no effect on the *R*-curve behaviour. Although significant residual stresses would be expected to be induced due to the differences in thermal expansion between the alumina and the crystallized intergranular phase, these appear to be relaxed by flow of residual glass. The results have interesting implications with respect to the applications of these materials, because they show that prolonged heat-treatment cycles up to 1200°C do not affect the room-temperature mechanical properties.

## Acknowledgements

The authors thank S. J. Bennison, B. R. Lawn and M. J. Readey for many stimulating and useful discussions, and B. R. Lawn for valuable suggestions regarding the manuscript. The authors also thank M. J. Readey, Coors Ceramics Co., for providing the starting materials. This work was funded jointly by Coors Ceramics Company and Air Force Office of Scientific Research.

## References

1. R. KNEHANS and R. W. STEINBRECH, *J. Mater. Sci. Lett.* **1** (1982) 327.
2. R. W. STEINBRECH, R. KNEHANS and W. SCHAAR-WACHTER, *J. Mater. Sci.* **18** (1983) 265.
3. R. F. COOK, B. R. LAWN and C. J. FAIRBANKS, *J. Amer. Ceram. Soc.* **68** (1985) 604.
4. M. V. SWAIN, *J. Mater. Sci. Lett.* **5** (1986) 1313.
5. A. REICHL and R. W. STEINBRECH, *J. Amer. Ceram. Soc.* **71** (1988) C299.
6. S. J. BENNISON and B. R. LAWN, *J. Mater. Sci.* **24** (1989) 3169.
7. K. KENDAL, N. McN. ALFORD, S. R. TAN and J. D. BIRCHALL, *J. Mater. Res.* **1** (1986) 120.
8. R. F. COOK and D. R. CLARKE, *Acta Metall.* **36** (1988) 555.
9. D. K. SHETTY and J. S. WANG, *J. Amer. Ceram. Soc.* **72** (1989) 1158.
10. P. L. SWANSON, C. J. FAIRBANKS, B. R. LAWN, Y.-W. MAI and B. J. HOCKEY, *ibid.* **70** (1987) 279.
11. S. J. BENNISON and B. R. LAWN, *Acta Metall.* **37** (1989) 2659.
12. Y.-W. MAI and B. R. LAWN, *J. Amer. Ceram. Soc.* **70** (1987) 289.
13. S. J. BENNISON, H. M. CHAN and B. R. LAWN, *ibid.* **72** (1989) 677.
14. N. A. TRAVITZKY, D. G. BRANDON and E. Y. GUTMANAS, *Mater. Sci. Engng* **71** (1985) 65.
15. *Idem.*, *ibid.* **71** (1985) 77.
16. Y. YESHURUN, Z. ROSENBERG, N. A. TRAVITZKY and D. G. BRANDON, *ibid.* **71** (1985) 71.
17. W. A. ZDANIEWSKI and H. P. KIRCHNER, *Adv. Ceram. Mater.* **1** (1986) 99.
18. H. TOMASZEWSKI, *Ceram. Int.* **14** (1988) 93.
19. C. A. POWELL-DOĞAN and A. H. HEUER, *J. Amer. Ceram. Soc.*, *J. Amer. Ceram. Soc.* **73** (1990) 3684.
20. D. B. MARSHALL, *Amer. Ceram. Soc. Bull.* **59** (1980) 551.
21. R. J. ROARK, in "Formulas for Stress and Strain" (McGraw-Hill, New York, 1965) Ch. 7.
22. S. M. WIEDERHORN, B. J. HOCKEY and R. F. KRAUSE Jr, in "Ceramic Microstructures '86", edited by J. Pask and A. G. Evans (Plenum, New York, 1988) p. 795.
23. L. KLEIN and D. R. UHLMANN, *J. Geophys. Res.* **79** (1974) 4869.
24. C. P. ALPERT, H. M. CHAN, S. J. BENNISON and B. R. LAWN, *J. Amer. Ceram. Soc.* **71** (1988) C371.
25. P. CHANTIKUL, S. J. BENNISON and B. R. LAWN, *ibid.*, **73** (1990) 2419.
26. D. WEYL, *Ber. Deut. Keram. Ges.* **36** (1959) 319.
27. J. SELSING, *J. Amer. Ceram. Soc.* **44** (1961) 419.
28. G. BAYER, *Proc. Brit. Ceram. Soc.* **22** (1973) 39.
29. M. CZANK and H. SCHULZ, *Naturwiss.* **54** (1971) 94.
30. J. V. SMITH and W. L. BROWN, in "Feldspar Minerals", Vol. 1 (Springer-Verlag, Berlin, 1988) Ch. 12.
31. N. BANSAL and R. H. DOREMUS, in "Handbook of Glass Properties" (Academic Press, Orlando, 1986) Ch. 9.

Received 20 March  
and accepted 5 July 1990